44th SLAC summer institute
Lecture III:
QCD parton model: Jets and Top

Keith Ellis
IPPP, Durham

August 17, 2016

Ingredients for a parton calculation

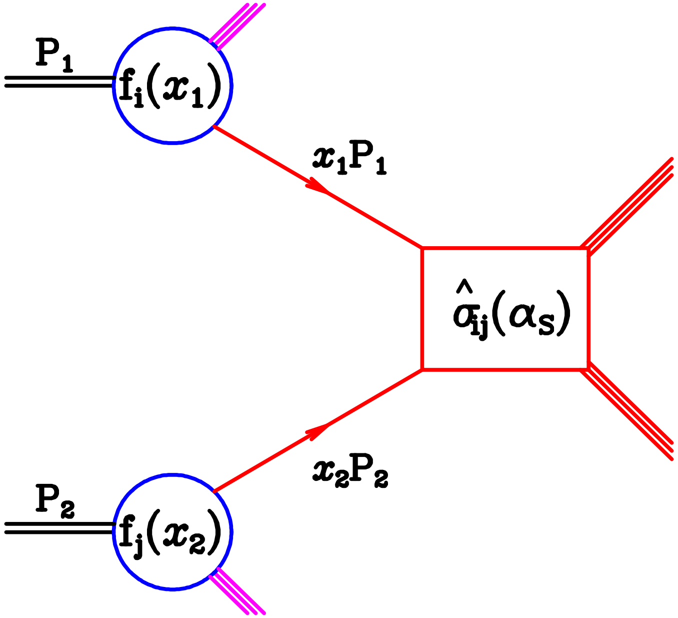

- Factorization formula

$$\sigma(S) = \sum_{i,j} \int dx_1 dx_2 f_i(x_1, \mu^2) f_j(x_2, \mu^2) \hat{\sigma}_{ij}(\hat{s} = x_1 x_2 S, \alpha_S(\mu^2), Q^2/\mu^2)$$

- Non-perturbative parton distributions $f_i(x, \mu^2)$ with calculable scale dependence.
- Short distance cross section that depends on α_s and factorization scale μ.
- Value of the coupling α_s with known scale dependence.

Parton luminosity

- Parton luminosity is determined by the parton distribution functions, $f_i(x_1,\mu^2)$ and $f_j(x_2,\mu^2)$.

- $f_j(x_i,\mu^2)$ need to be determined by data.
- the available centre-of-mass energy-squared of the parton-parton collision, $\hat{s}$, is less than the overall hadron-hadron collision energy, s, by a factor of $x_1 x_2 \equiv \tau$.
- Define differential parton luminosities

$$\tau \frac{dL_{ij}}{d\tau} = \frac{1}{1+\delta_{ij}} \int_0^1 dx_1 dx_2$$

$$\times \Big[\big(x_1 f_i(x_1,\mu^2)\; x_2 f_j(x_2,\mu^2) \big) + (1 \leftrightarrow 2) \Big] \delta(\tau - x_1 x_2).$$

- The collider luminosity is quite distinct from the parton luminosity. The former is a property of a machine, whereas the latter is a property of the proton.
- We now assume that $\hat{\sigma}$ depends only on $\hat{s}$.

$$\sigma(s) = \sum_{\{ij\}} \int_{\tau_0}^1 \frac{d\tau}{\tau} \left[\frac{1}{s} \frac{dL_{ij}}{d\tau} \right] \left[\hat{s} \hat{\sigma}_{ij} \right],$$

Parton luminosity

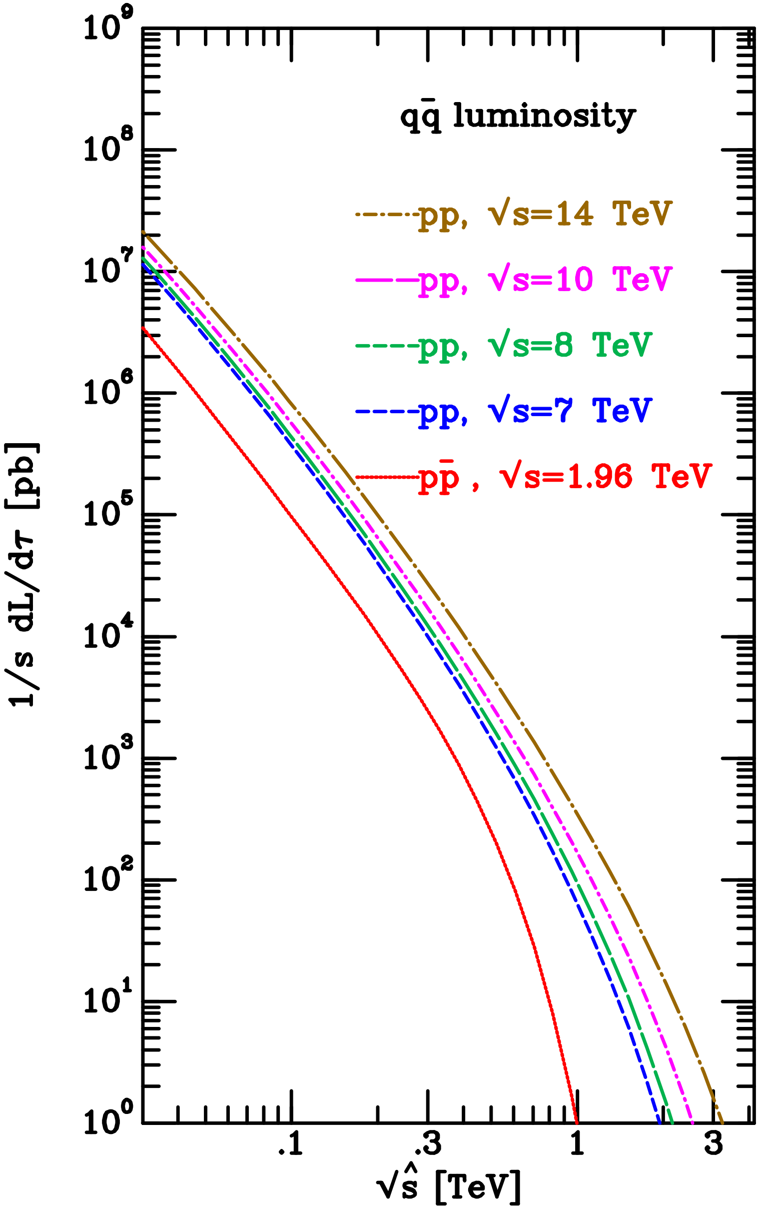

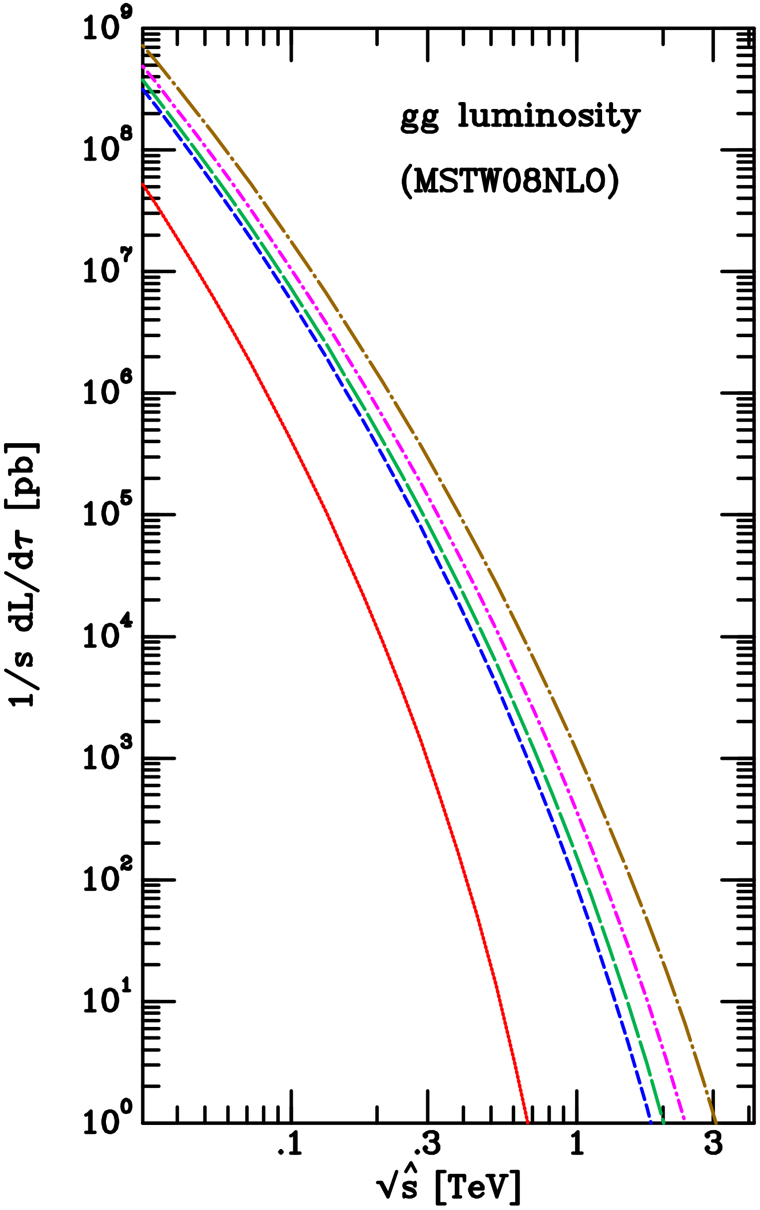

Ratios of luminosities

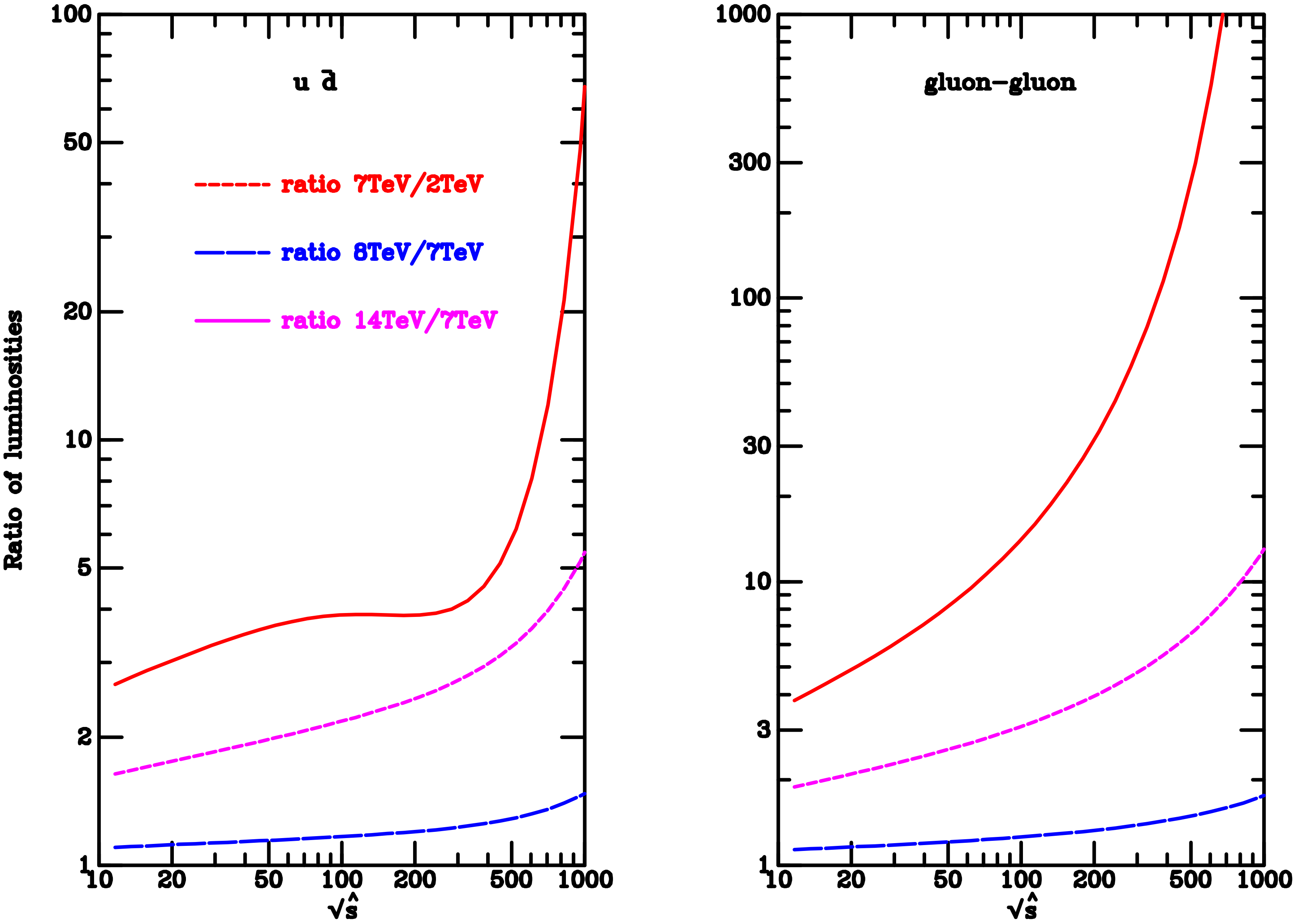

Jet physics

- There is little doubt that jet physics displays fundamental scattering of constituents.
- Probes pointlike behaviour on shortest distance scales.
- But what is a jet?

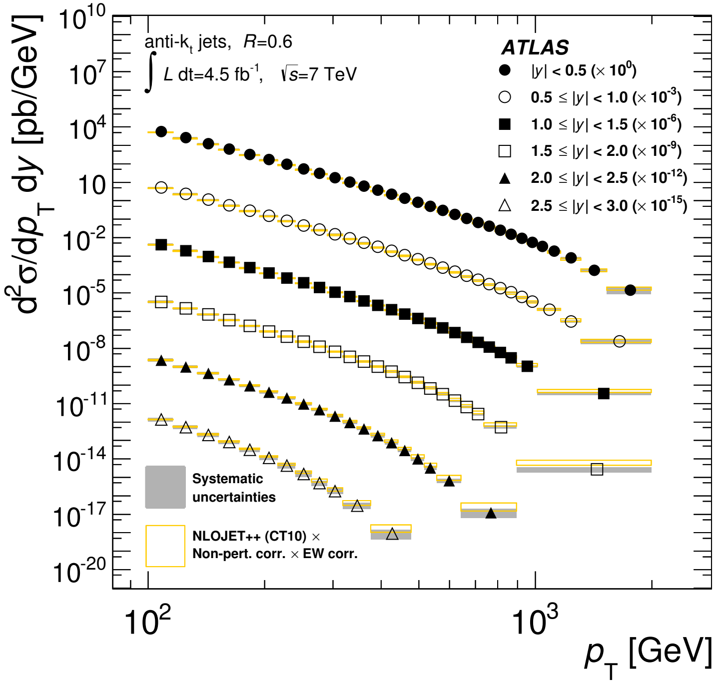

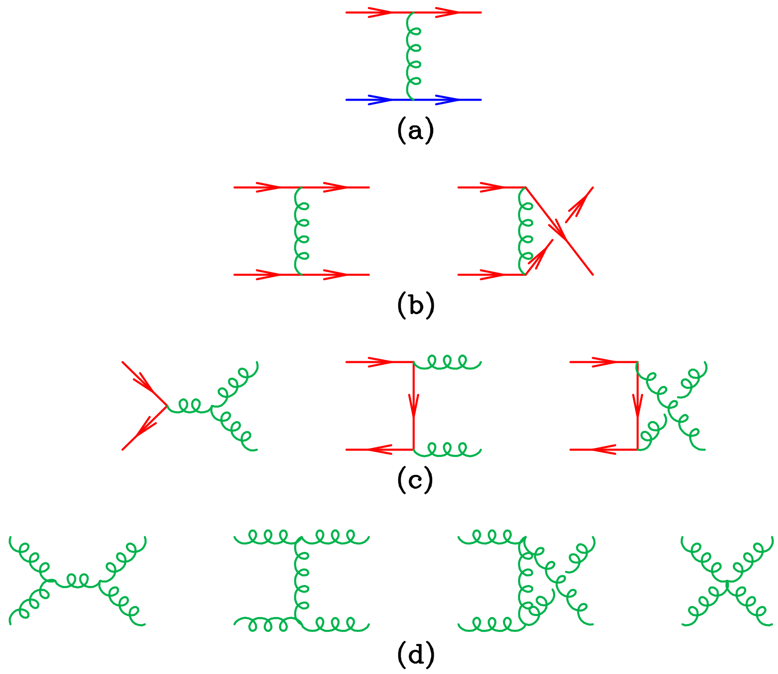

Jet algorithms

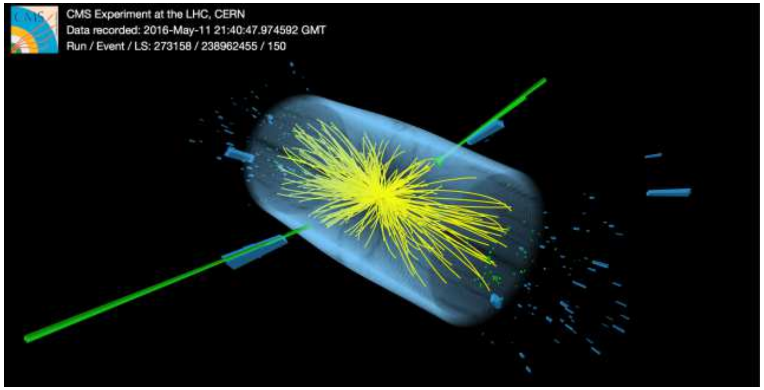

- Jet structure is obvious to the naked eye;
- A jet definition is like a legal contract between theorists and experimenters; many contracts are possible, different contracts are useful in different circumstances, but all contracts must be defined precisely
- a jet definition requires:-
  - ☐ a jet algorithm
  - ☐ jet parameters, e.g. a cone size R
  - ☐ a recombination scheme for combining entities
- Desirable properties; infrared safety, speed, defined jet area for subtraction of pile up and underlying event.
- Two types of jet algorithms.
  - ☐ Sequential recombination algorithm
  - ☐ Cone algorithms

The two classes of jet algorithms

- Sequential recombination algorithms
  - Combine entities (particles) starting with the closest ones
  - Requires definition of close, (distance measure)
  - Iterate recombination until there are few entities (jets) left
  - Examples, Jade, k_t,Cambridge/Aachen, anti-k_t
- Cone algorithms
  - Identify regions with large energy flow
  - Cone algorithms give rise to regular jets which are easier to calibrate, and to remove underlying event.
  - Examples, ATLAS cone, CMS cone, SIScone

I shall only talk about sequential recombination algorithms in the following.

Sequential recombination jet algorithms

- introduce distances (d_{ij}) between entities (particles, pseudojets) i and j and between an entity and the beam (d_{iB})

$$d_{ij} = \min(k_{t\,i}^{2p}, k_{t\,i}^{2p})\frac{\Delta R_{ij}^2}{R^2}, \quad d_{iB} = k_{t\,i}^{2p}$$

$$\Delta R_{ij}^2 = (y_i - y_j)^2 + (\phi_i - \phi_j)^2$$

- $k_{t\,i}, y_i, \phi_i$ are the transverse momentum, rapidity and azimuth of entity i
- Clustering proceeds by identifying the smallest of the distances;
  - ☐ if it is d_{ij} recombine entities i and j;
  - ☐ if it is d_{iB}, call i a jet and remove it from the list of entities to be clustered.
  - ☐ iterate
- Note that entities separated in angle, such that $\Delta R_{ij}^2 > R^2$ will never be clustered.
- Sequential recombination algorithms return not only a list of jets, but also a clustering sequence, which contains valuable information about the morphology of the event.

Infrared safety of k_t algorithms

- introduce distances between entities (particles, pseudojets) i and j (d_{ij}) and between an entity and the beam (d_{iB})

$$d_{ij} = \min(k_{t\,i}^{2p}, k_{t\,i}^{2p})\frac{\Delta R_{ij}^2}{R^2}, \quad d_{iB} = k_{t\,i}^{2p}$$

- Establish IR safety by asking how clustering sequence would change, with the addition of soft or collinear radiation.
  - ☐ emission of a collinear particle, $\Delta y^2 + \Delta\phi^2 \to 0$ in all cases means that the jet measure $d_{ij} \to 0$. Hence collinearly emitted particles are clustered first, leaving resultant jets unchanged.
    - for p=1, a new soft particle, $k_{t\,i} \to 0$ gives the smallest d_{ij}, hence clustered first leaving jets unchanged.
    - for p=0, a new soft particle can be a new jet of zero momentum, leaving hard jets unchanged
    - for p=-1, a new soft particle $k_{t\,i} \to 0$ gives the largest $d_{ij} \to \infty$, clustered last or new zero-momentum jet, leaving hard jets unchanged.

Jet algorithms compared

Jet algorithm	distance measure	Authors	Scaling
SIScone	Seedless iterative cone with split-merge	Salam et al, 0704.0292	$N^2 \ln N$
k_t	$d_{ij} = \min(k_{ti}^2, k_{ti}^2)\Delta_{ij}/R^2$, Ordered in k_t	Catani et al,NPB406 (1993) S.Ellis et al, 9305266	$N \ln N$
Cambridge/ Aachen	$d_{ij} = \Delta_{ij}/R^2$, Ordered in angle	Dokshitzer et al,9907280 Wengler et al, 9907280	$N \ln N$
anti-k_t	$d_{ij} = \min(k_{ti}^{-2}, k_{ti}^{-2})\Delta_{ij}/R^2$, Gives conical hard jets	Cacciari et al, 0802.1189	$N^{3/2}$

- Siscone, Seedless infra-red safe algorithm
- Infrared safety is both a theoretical necessity and an exprimental imperative.

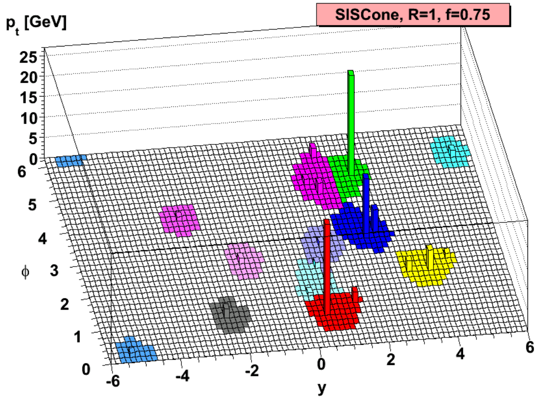

Sequential recombination jet algorithms compared

- k_t algorithm ($p=1$); d_{ij} distance measure is the inverse of the branching probability, (the pair which is recombined first is the one with the largest probability to have branched last). The clustering sequence has a physical meaning. Helpful for theoretical resummation.

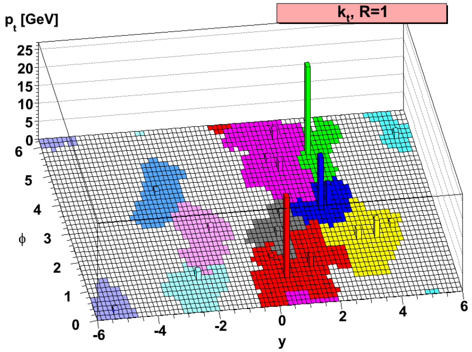

- C/A algorithm ($p=0$); still contains features of the parton shower because of the angular ordering property of QCD radiation; it is a compromise between the structure of the parton shower and limiting the sensitivity to soft radiation.

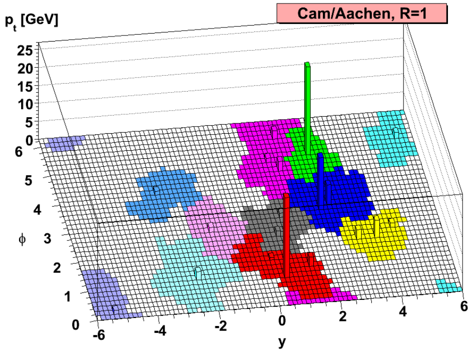

- the anti-k_t algorithm ($p=-1$); soft radiation is always clustered last; gives rise to approximately conical jets. A bizarre choice, which nevertheless gives very useful jets for pileup and underlying event subtraction.

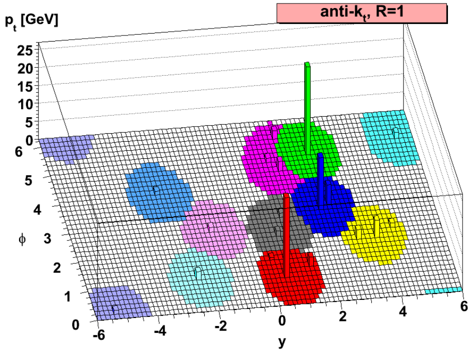

Branching kinematics

$$
\begin{aligned}
a^\mu &= p^\mu + \frac{\mathbf{p}_T^2 + m^2}{2} n^\mu + \mathbf{p}_T^\mu \\
b^\mu &= z p^\mu + \frac{\mathbf{b}_T^2}{2z} n^\mu + \mathbf{b}_T^\mu \\
c^\mu &= (1-z) p^\mu + \frac{\mathbf{c}_T^2}{2(1-z)} n^\mu + \mathbf{c}_T^\mu
\end{aligned}
$$

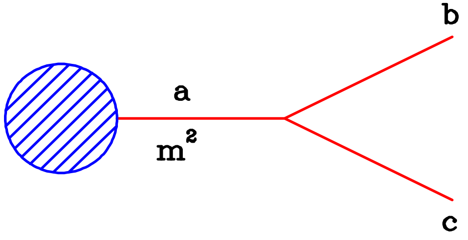

$$a = b + c$$

where $n \cdot p = 1, p \cdot p = n \cdot n = 0$,
$p \cdot \mathbf{x}_T = n \cdot \mathbf{x}_T = 0$. Setting

$$\mathbf{b}_T = z\mathbf{p}_T + \mathbf{k}_T, \quad \mathbf{c}_T = (1-z)\mathbf{p}_T - \mathbf{k}_T$$

we find in the small $\mathbf{k}_T$ approximation that

$$(y_b - y_c)^2 = \frac{(\mathbf{p}_T \cdot \mathbf{k}_T)^2}{\mathbf{p}_T^2 z^2 (1-z)^2}$$

$$a^2 = m^2 \approx \frac{\mathbf{k}_T^2}{z(1-z)}, \quad \Delta R_{bc}^2 = (y_b - y_c)^2 + (\phi_b - \phi_c)^2 \approx \frac{m^2}{z(1-z)\mathbf{p}_T^2}$$

$$\Delta y_{bc}^2 = \frac{\min\{\mathbf{b}_T^2, \mathbf{c}_T^2\}}{m^2} \times \Delta R_{bc}^2 \simeq \frac{z}{1-z}, \quad \text{for } z < \frac{1}{2}$$

Jet mass

Ingredients for a parton calculation
Parton luminosity
Jet physics
Jet algorithms
Branching kinematics
Higgs and QCD branchings compared: angular separation
Higgs and QCD branchings compared: mass drop
Separating signal and background in $VH(\to b\bar{b})$
Higgs tagging-filtering
Why top?
LO Top production
NLO Heavy quark production
Scale dependence
NNLO
Top @NNLO
NNLO top
Recap
Bibliography

- In the collinear approximation the amplitude to radiate an extra parton can be written as

$$d\sigma_{n+1} \approx d\sigma_n \, dz \, \frac{dt}{t} \, \frac{\alpha_s}{2\pi} \, P(z),$$

- $m^2 = t$ is the jet mass, and z is the longitudal momentum branching fraction. The splitting function $P(z)$ for $q \to gq$ is

$$P_{gq}(z) = C_F \, \frac{1+(1-z)^2}{z}.$$

$$\langle m^2 \rangle = \langle t \rangle \approx \int_0^1 dz \int_0^{t_{\max}} \frac{dt}{t} \, t \, \frac{\alpha_s}{2\pi} P_{gq}(z).$$

The jet algorithm imposes that $\Delta R_{bc} < R$, and hence that $t_{\max} = \mathbf{p}_T^2 R^2 z(1-z)$.

- taking a fixed α_s for the moment we see that

$$\langle m^2 \rangle \approx \mathbf{p}_T^2 R^2 \, \frac{\alpha_s}{2\pi} \int dz \, z(1-z) \, P_{bc}(z).$$

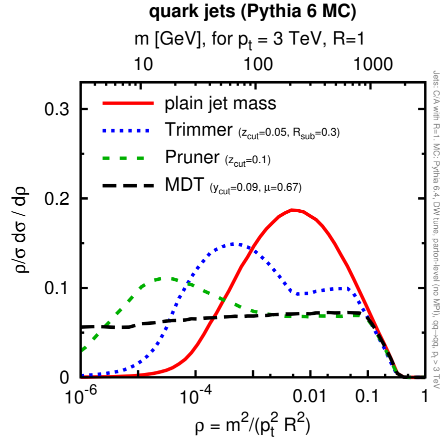

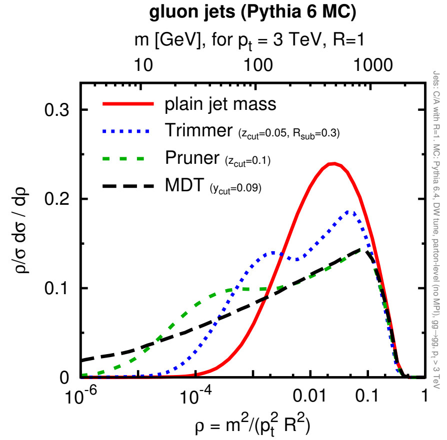

- leading to the conclusion $\langle m^2 \rangle \propto \mathbf{p}_T^2 R^2 \, \frac{\alpha_s}{2\pi} C_F / C_A$.
- Plots display Casimir broadening

Higgs and QCD branchings compared: angular separation

- From the kinematics of branching alone, we have established that

$$\sqrt{\Delta R_{ij}^2} \sim \frac{m}{p_T} \frac{1}{\sqrt{z(1-z)}} \sim \frac{2m}{p_T}.$$

- Evaluate the distance measure y_{bc} in the presence of a splitting function $P \to bc$:

$$y_{bc} = \frac{\min(\mathbf{b}_T^2, \mathbf{c}_T^2)}{m^2} \times \Delta R_{bc}^2 \approx \frac{p_T^2 z^2}{m^2} \times \frac{m^2}{p_T^2 z(1-z)} \approx \frac{z}{1-z}.$$

At fixed jet mass this is the result for the decay of a Higgs boson. QCD jets give rise to a different result, especially because of the $1/z$-behaviour.

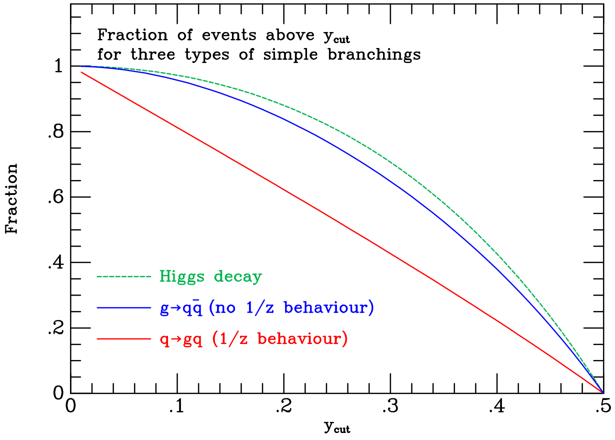

$$\begin{aligned} P_{h\to b\bar{b}} &\propto 1 \\ P_{q\to gq} &\propto \frac{1+(1-z)^2}{z} \\ P_{g\to q\bar{q}} &\propto z^2+(1-z)^2 \end{aligned}$$

Higgs and QCD branchings compared: mass drop

- A boosted Higgs with mass m_H, decays to (essentially) massless daughters in one step;
- QCD splittings favour slower degradation in the virtuality.
- the Sudakov form factor expresses the probability of evolving from an initial virtuality t_0 to a final virtuality t without branching:

$$\Delta(t) = \exp\left[-\int_{t_0}^{t} \frac{dt'}{t'}\, dz \frac{\alpha_s}{2\pi} P(z)\right].$$

- In the fixed coupling constant approximation we find that,

$$\Delta(t) \propto \left(\frac{t_0}{t}\right)^p$$

- for $p > 0$, $\Delta(t) \to 0$ for large t. The probability of a QCD jet arriving at mass squared t_0, from a large mass squared t falls like a positive power of (t_0/t)

Separating signal and background in $VH(\to b\bar{b})$

- A Higgs boson H decaying to $b\bar{b}$ differs in two ways from a QCD branching
  - ☐ the splitting will be symmetric,
  - ☐ the jet mass fill drop faster in the branching

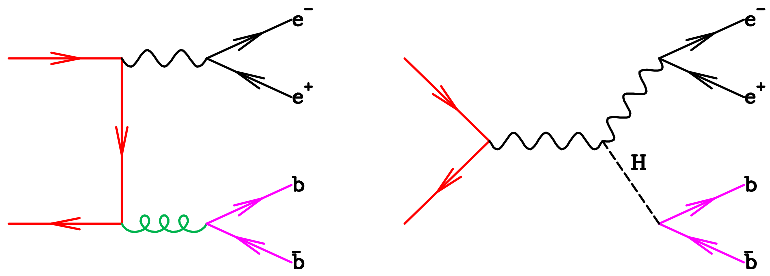

Background **Signal**

- the BDRS procedure (arXiv:0802.2470) exploits these two features
- First cluster the event on a large angular scale, $R_{b\bar{b}}$, using the Cambridge-Aachen jet definition. (The clustering scale of $R_{b\bar{b}}$ is set by $2m/|\mathbf{p}_T|$).
- Undo the cluster sequence one branching at a time and check on the mass drop and symmetry of the branching, to identify whether the branching belongs in the Higgs neighbourhood. The declustering involves two dimensionless parameters, μ (0.67) and $y_{\rm cut}$ (0.09):

$$\max(m_i, m_j) < \mu m_P(\text{massdrop}), \quad y_{ij} > y_{cut}(\text{symmetric})$$

- Continue until either a Higgs-like branching has been identified or no jets remain.

Higgs tagging-filtering

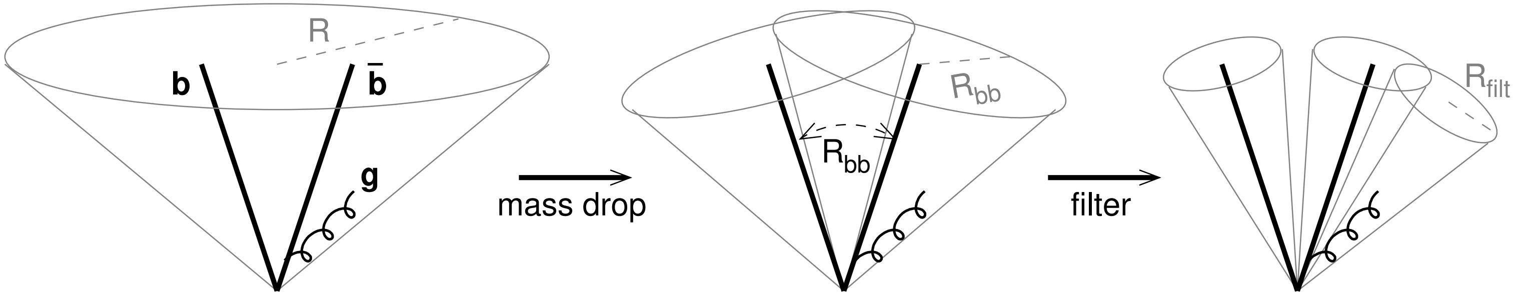

- Filter the Higgs neighbourhood, by clustering the events on a smaller angular scale $R_{\rm filt} < R_{b\bar{b}}$ and keep only the three hardest subjets (to allow for $b, \bar{b}$ and possible parton radiation).
- This step helps to remove pile-up.
- MC results for 30 fb^{-1} (a) e^+e^- or $\mu^+\mu^-$ (b) lepton + Missing transverse momentum (c) Missing transverse momentum (d) All channels

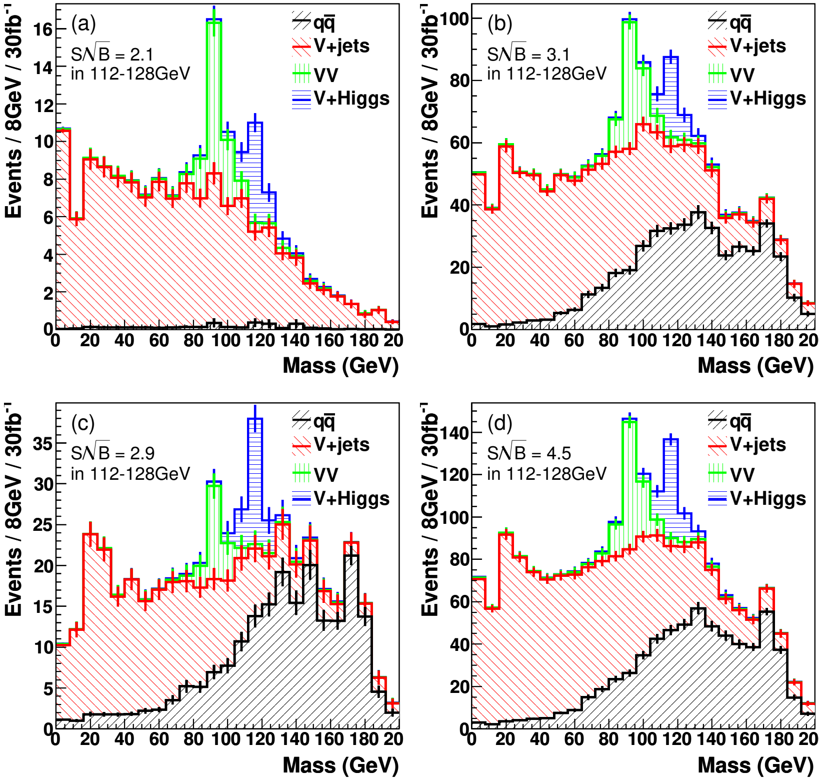

Why top?

- The top quark cross section is large at LHC energies, one event in 10^6
- Since $m_t > M_W + m_b$ a top quark decays predominantly into a b quark and an on-shell W boson

$$\begin{aligned} t &\to W^+ + b \\ &\qquad \hookrightarrow l^+ + \nu \end{aligned}$$

$$\begin{aligned} t &\to W^+ + b \\ &\qquad \hookrightarrow q + \bar{q} \end{aligned}$$

- In the limit $m_t \gg M_W$ the result for the total width is

$$\Gamma(t \to bW) = \frac{G_F m_t^3}{8\pi\sqrt{2}} |V_{tb}|^2 \approx 1.76\ \mathrm{GeV} \left(\frac{m_t}{175\ \mathrm{GeV}} \right)^3 .$$

$V_{tb} \approx 1$ as suggested by the unitarity relation $|V_{tb}|^2 + |V_{cb}|^2 + |V_{ub}|^2 = 1.$

- The top quark decays before it has time to hadronize.
- The top is a copious source of b's and W's

LO Top production

- The leading-order processes for the production of a heavy quark Q of mass m in hadron-hadron collisions

$$\begin{array}{ll} (a) & q(p_1)+\overline{q}(p_2)\to Q(p_3)+\overline{Q}(p_4) \\ (b) & g(p_1)+g(p_2)\to Q(p_3)+\overline{Q}(p_4) \end{array}$$

where the four-momenta of the partons are given in brackets ($\rho = 4m^2/s$).

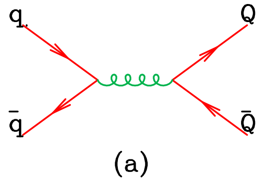

(a)

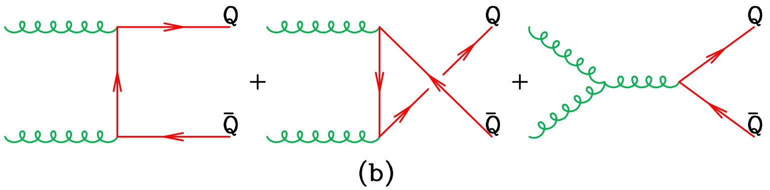

(b)

Process	$\overline{\sum}\vert\mathcal{M}\vert^2/g^4$
$q\,\overline{q}\to Q\,\overline{Q}$	$\frac{4}{9}\left(\tau_1^2+\tau_2^2+\frac{\rho}{2}\right)$
$g\,g\to Q\,\overline{Q}$	$\left(\frac{1}{6\tau_1\tau_2}-\frac{3}{8}\right)\left(\tau_1^2+\tau_2^2+\rho-\frac{\rho^2}{4\tau_1\tau_2}\right)$

- The matrix elements squared have been averaged (summed) over initial (final) colours and spins, as indicated by $\overline{\sum}$.
- We have introduced the following notation for the ratios of scalar products:

$$\tau_1 = \frac{2p_1.p_3}{\hat{s}},\quad \tau_2 = \frac{2p_2.p_3}{\hat{s}},\quad \rho = \frac{4m^2}{\hat{s}},\quad \hat{s} = (p_1+p_2)^2.$$

Differential distributions

- The short-distance cross section is obtained from the invariant matrix element in the usual way:

$$d\hat{\sigma}_{ij} = \frac{1}{2\hat{s}} \frac{d^3p_3}{(2\pi)^3 2E_3} \frac{d^3p_4}{(2\pi)^3 2E_4} (2\pi)^4 \delta^4(p_1+p_2-p_3-p_4) \overline{\sum} |\mathcal{M}_{ij}|^2 .$$

  The first factor is the flux factor for massless incoming particles. The other terms come from the phase space for $2 \to 2$ scattering.
- In terms of the rapidity $y = \frac{1}{2}\ln((E+p_z)/(E-p_z))$ and transverse momentum, p_T, the relativistically invariant phase space volume element of the final-state heavy quarks is

$$\frac{d^3p}{E} = dy \; d^2p_T \; .$$

  The result for the invariant cross section may be written as

$$\frac{d\sigma}{dy_3 dy_4 d^2p_T} = \frac{1}{16\pi^2 \hat{s}^2} \sum_{ij} x_1 f_i(x_1,\mu^2) \; x_2 f_j(x_2,\mu^2) \overline{\sum} |\mathcal{M}_{ij}|^2 .$$

  x_1 and x_2 are fixed if we know the transverse momenta and rapidity of the outgoing heavy quarks.

Differential distributions

- In the centre-of-mass system of the incoming hadrons we may write

$$\begin{aligned}
p_1 &= \frac{1}{2}\sqrt{s}(x_1, 0, 0, x_1) \\
p_2 &= \frac{1}{2}\sqrt{s}(x_2, 0, 0, -x_2) \\
p_3 &= (m_T \cosh y_3, p_T, 0, m_T \sinh y_3) \\
p_4 &= (m_T \cosh y_4, -p_T, 0, m_T \sinh y_4).
\end{aligned}$$

Applying energy and momentum conservation, we obtain

$$\begin{aligned}
x_1 &= \frac{m_T}{\sqrt{s}}(e^{y_3} + e^{y_4}) \\
x_2 &= \frac{m_T}{\sqrt{s}}(e^{-y_3} + e^{-y_4}) \\
\hat{s} &= 2m_T^2(1 + \cosh \Delta y).
\end{aligned}$$

The quantity $m_T = \surd(m^2 + p_T^2)$ is the transverse mass of the heavy quarks and $\Delta y = y_3 - y_4$ is the rapidity difference between them.

Differential distributions

- In these variables the leading order cross section is

$$\frac{d\sigma}{dy_3 dy_4 d^2 p_T} = \frac{1}{64\pi^2 m_T^4 (1+\cosh(\Delta y))^2} \times \sum_{ij} x_1 f_i(x_1,\mu^2)\, x_2 f_j(x_2,\mu^2) \overline{\sum} |\mathcal{M}_{ij}|^2 .$$

Expressed in terms of m, m_T and Δy, the matrix elements for the two processes are

$$\overline{\sum}|\mathcal{M}_{q\bar{q}}|^2 = \frac{4g^4}{9}\left(\frac{1}{1+\cosh(\Delta y)}\right)\left(\cosh(\Delta y) + \frac{m^2}{m_T^2}\right) ,$$

$$\overline{\sum}|\mathcal{M}_{gg}|^2 = \frac{g^4}{24}\left(\frac{8\cosh(\Delta y)-1}{1+\cosh(\Delta y)}\right)\left(\cosh(\Delta y) + 2\frac{m^2}{m_T^2} - 2\frac{m^4}{m_T^4}\right).$$

- As the rapidity separation Δy between the two heavy quarks becomes large

$$\overline{\sum}|\mathcal{M}_{q\bar{q}}|^2 \sim \text{ constant}, \quad \overline{\sum}|\mathcal{M}_{gg}|^2 \sim \exp \Delta y \ .$$

- The cross section is damped at large Δy and heavy quarks produced by $q\bar{q}$ annihilation are more closely correlated in rapidity those produced by gg fusion.

Applicability of perturbation theory?

- Consider the propagators in the diagrams.

$$\begin{aligned}(p_1+p_2)^2 &= \quad 2p_1.p_2 \quad &&= 2m_T^2\left(1+\cosh\Delta y\right)\ ,\\ (p_1-p_3)^2-m^2 &= \quad -2p_1.p_3 \quad &&= -m_T^2\left(1+e^{-\Delta y}\right)\ ,\\ (p_2-p_3)^2-m^2 &= \quad -2p_2.p_3 \quad &&= -m_T^2\left(1+e^{\Delta y}\right)\ .\end{aligned}$$

  Note that the propagators are all off-shell by a quantity of least of order m^2.
- Thus for a sufficiently heavy quark we expect the methods of perturbation theory to be applicable. It is the mass m (which by supposition is very much larger than the scale of the strong interactions Λ) which provides the large scale in heavy quark production. We expect corrections of order Λ/m
- This does not address the issue of whether the charm or bottom mass is large enough to be adequately described by perturbation theory.

NLO Heavy quark production

In NLO heavy quark production m is the heavy quark mass.

$$\sigma(S) = \sum_{i,j} \int dx_1 dx_2 \, \hat{\sigma}_{ij}(x_1 x_2 S, m^2, \mu^2) F_i(x_1, \mu^2) F_j(x_2, \mu^2)$$

$$\hat{\sigma}_{i,j}(\hat{s}, m^2, \mu^2) = \sigma_0 c_{ij}(\hat{\rho}, \mu^2)$$

where $\hat{\rho} = 4m^2/\hat{s}, \bar{\mu}^2 = \mu^2/m^2, \sigma_0 = \alpha_S^2(\mu^2)/m^2$ and $\hat{s}$ in the parton total c-of-m energy squared. The coupling satisfies

$$\frac{d\alpha_S}{d\ln\mu^2} = -b_0 \frac{\alpha_S^2}{2\pi} + O(\alpha_S^3), \;\; b_0 = \frac{11N - 2n_f}{6}$$

$$c_{ij}\left(\rho, \frac{\mu^2}{m^2}\right) = c_{ij}^{(0)}(\rho) + 4\pi\alpha_S(\mu^2)\left[c_{ij}^{(1)}(\rho) + \bar{c}_{ij}^{(1)}(\rho)\ln\left(\frac{\mu^2}{m^2}\right)\right] + O(\alpha_S^2)$$

The lowest-order functions $c_{ij}^{(0)}$ are obtained by integrating the lowest order matrix elements

$$c_{q\bar{q}}^{(0)}(\rho) = \frac{\pi\beta\rho}{27}\Big[(2+\rho)\Big], \quad c_{gq}^{(0)}(\rho) = c_{g\bar{q}}^{(0)}(\rho) = 0 \;,$$

$$c_{gg}^{(0)}(\rho) = \frac{\pi\beta\rho}{192}\left[\frac{1}{\beta}\left[\rho^2 + 16\rho + 16\right]\ln\left(\frac{1+\beta}{1-\beta}\right) - 28 - 31\rho\right] \,,$$

NLO Heavy quark production

- The functions $c_{ij}^{(1)}$ are also known
- In order to calculate the c_{ij} in perturbation theory we must perform both renormalization and factorization of mass singularities. The subtractions required for renormalization and factorization are done at mass scale μ.

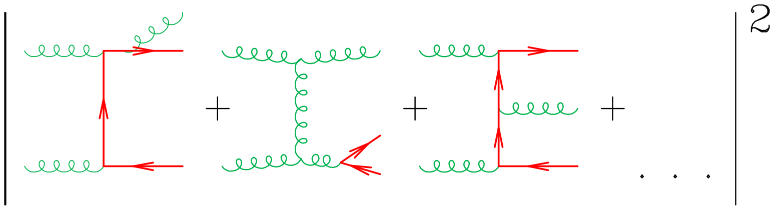

Real emission diagrams

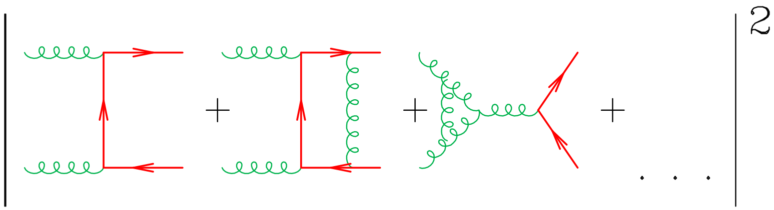

Virtual emission diagrams

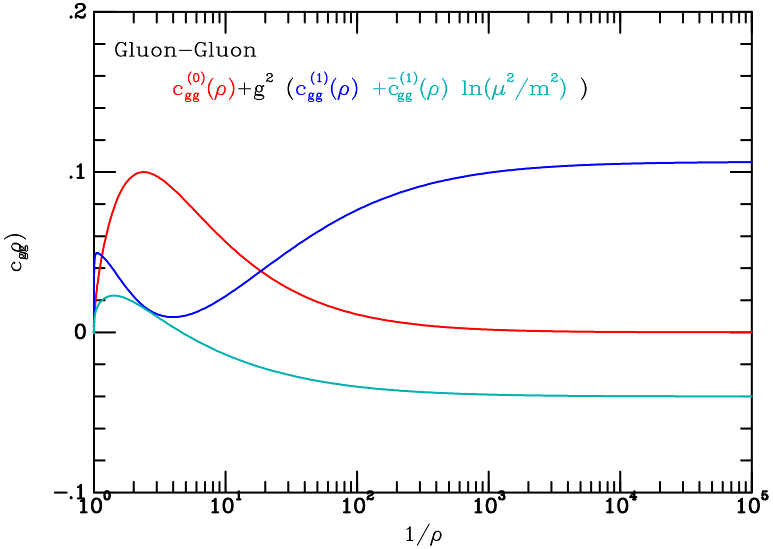

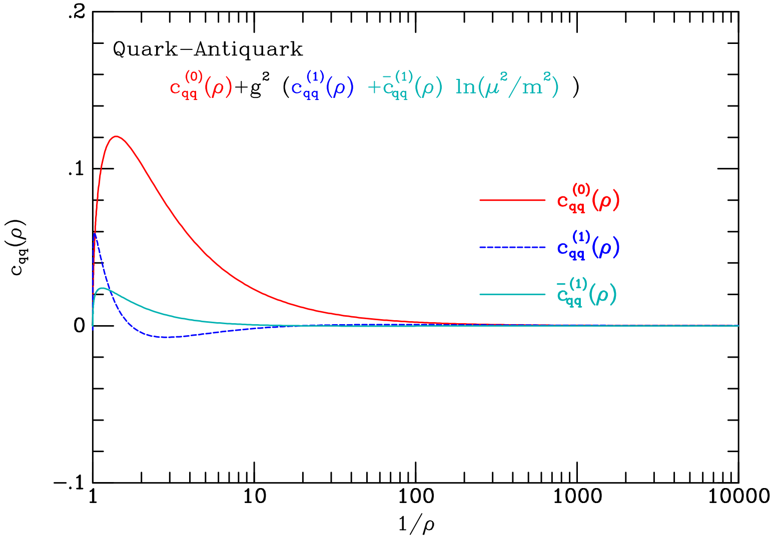

Scale dependence

μ is an unphysical parameter. The physical predictions should be invariant under changes of μ at the appropriate order in perturbation theory. If we have performed a calculation to $O(\alpha_S^3)$, variations of the scale μ will lead to corrections of $O(\alpha_S^4)$,

$$\mu^2 \frac{d}{d\mu^2}\sigma = O(\alpha_S^4).$$

- The term $\overline{c}^{(1)}$, which controls the μ dependence of the higher-order perturbative contributions, is fixed in terms of the lower-order result $c^{(0)}$:

$$\begin{aligned} \overline{c}_{ij}^{(1)}(\rho) &= \frac{1}{8\pi^2}\Bigg[4\pi b c_{ij}^{(0)}(\rho) - \int_\rho^1 dz_1 \sum_k c_{kj}^{(0)}(\frac{\rho}{z_1}) P_{ki}^{(0)}(z_1) \\ &- \int_\rho^1 dz_2 \sum_k c_{ik}^{(0)}(\frac{\rho}{z_2}) P_{kj}^{(0)}(z_2)\Bigg]. \end{aligned}$$

Scale dependence

- In obtaining this result we have used the renormalization group equation for the running coupling

$$\mu^2 \frac{d}{d\mu^2} \alpha_S(\mu^2) = -b\alpha_S^2 + \ldots$$

and the lowest-order form of the DGLAP equation

$$\mu^2 \frac{d}{d\mu^2} f_i(x,\mu^2) = \frac{\alpha_S(\mu^2)}{2\pi} \sum_k \int_x^1 \frac{dz}{z} P_{ik}^{(0)}(z) f_k(\frac{x}{z},\mu^2) + \ldots .$$

Scale dependence

- This illustrates an important point which is a general feature of renormalization group improved perturbation series in QCD.
- The coefficient of the perturbative correction depends on the choice made for the scale μ, but the scale dependence changes the result in such a way that the physical result is independent of that choice.
- Thus the scale dependence is formally small because it is of higher order in α_S.
- This does not assure us that the scale dependence is actually *numerically* small for all series.
- A pronounced dependence on the scale μ is a signal of an untrustworthy perturbation series.

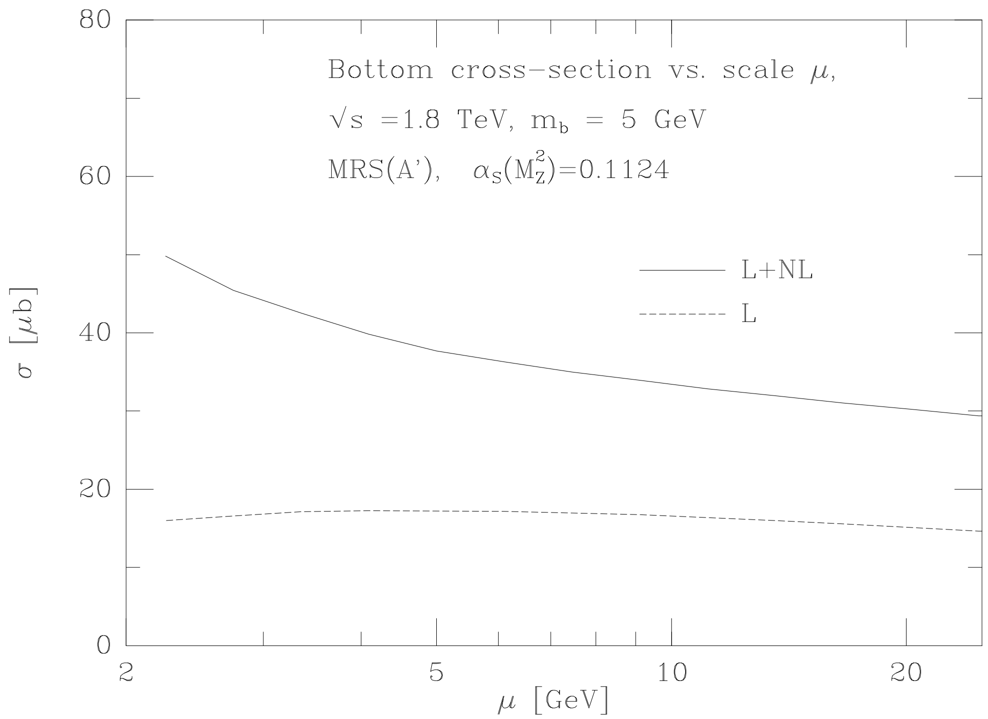

Scale dependence of top cross section

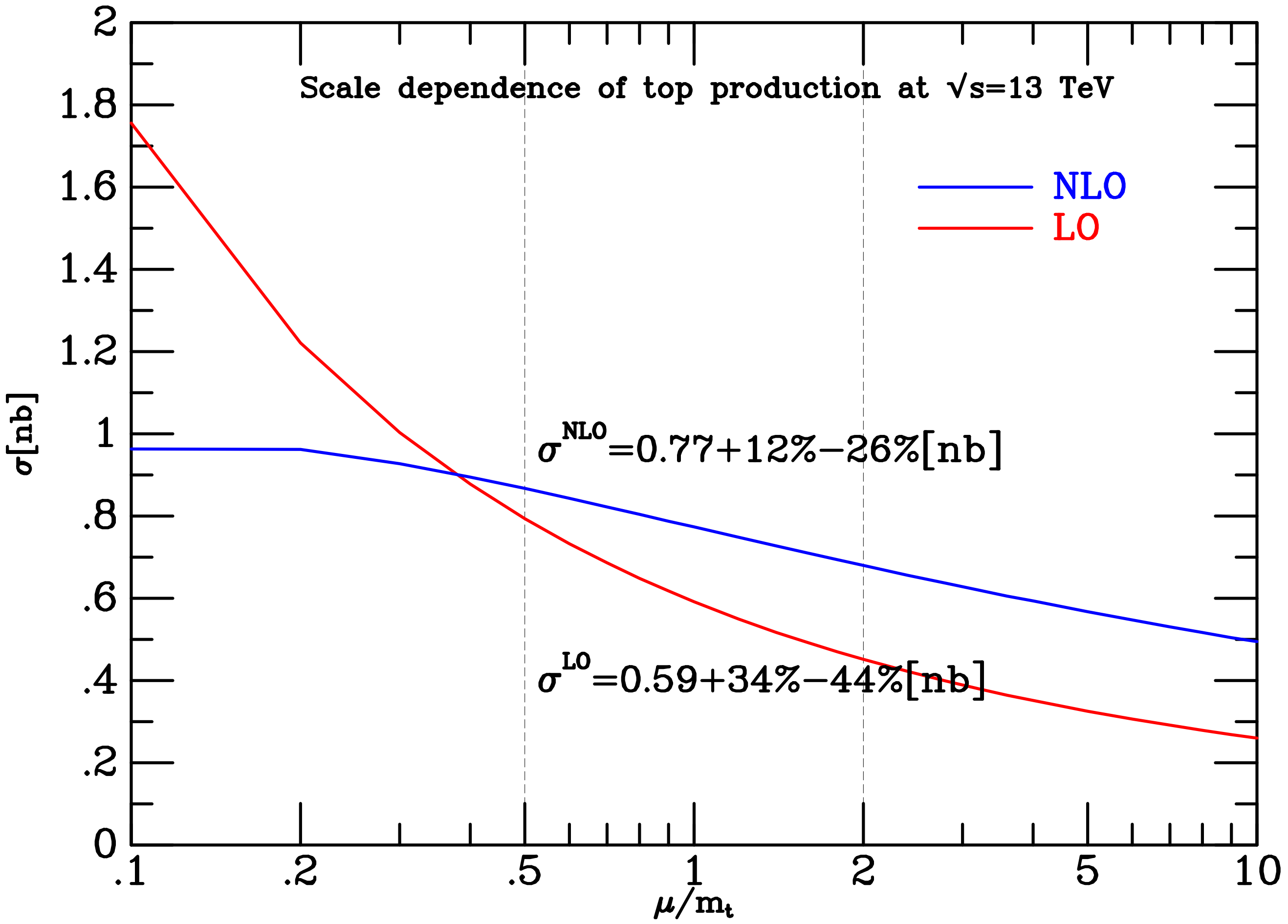

- Note that despite the fact that α_S is of order 10%, we do not obtain 10% predictions at NLO.
- This is 'feature' of renormalization group improved perturbation theory.

NNLO

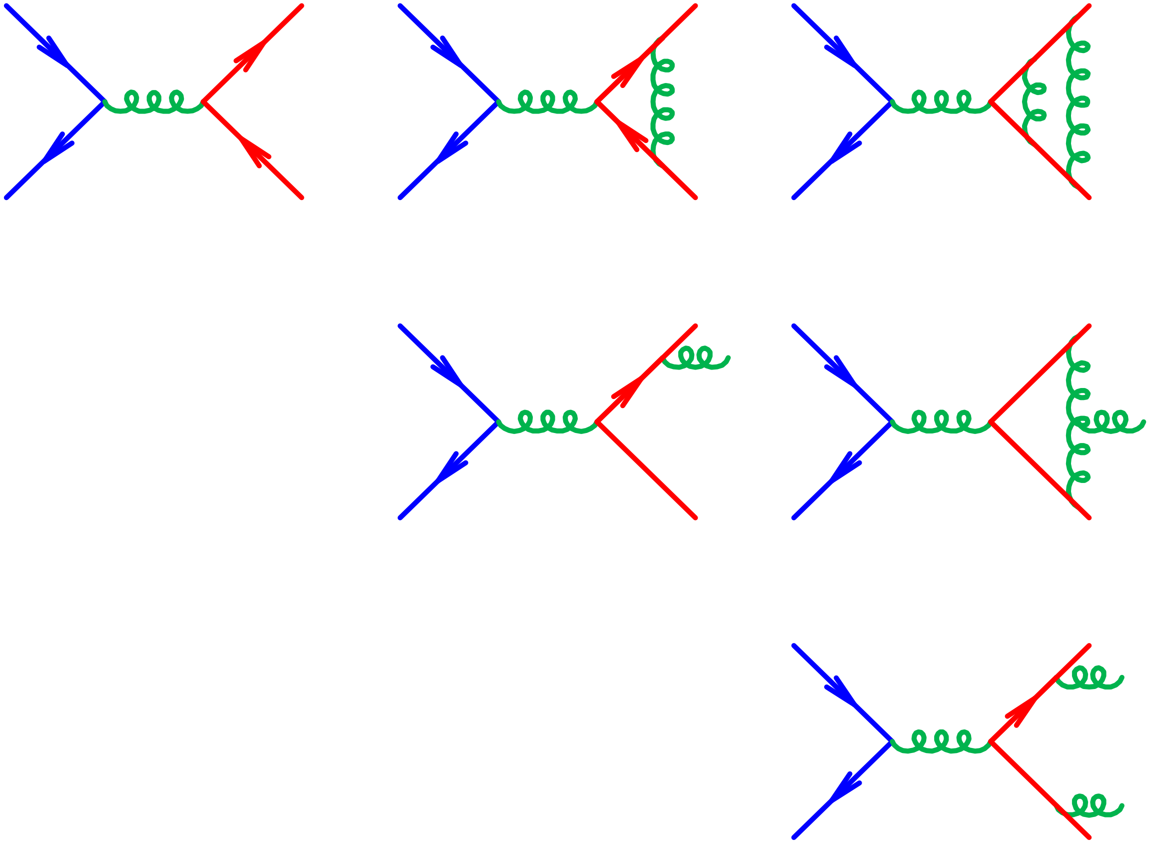

- Challenge is not the calculation of the individual diagrams, but rather the assembly of pieces that individually contain infrared divergences
- as before in the NLO calculations, tension between the need to cancel infra-red divergences, which for the higher multiplicity processes are only manifest after integration and the desire to have a fully differential prediction.

Top @NNLO

arXiv:1303.6254

Collider	σ_{tot} [pb]	scales [pb]	pdf [pb]
Tevatron	7.164	$+0.110(1.5\%)$ $-0.200(2.8\%)$	$+0.169(2.4\%)$ $-0.122(1.7\%)$
LHC 7 TeV	172.0	$+4.4(2.6\%)$ $-5.8(3.4\%)$	$+4.7(2.7\%)$ $-4.8(2.8\%)$
LHC 8 TeV	245.8	$+6.2(2.5\%)$ $-8.4(3.4\%)$	$+6.2(2.5\%)$ $-6.4(2.6\%)$
LHC 14 TeV	953.6	$+22.7(2.4\%)$ $-33.9(3.6\%)$	$+16.2(1.7\%)$ $-17.8(1.9\%)$

Table 1: Best NNLO+NNLL theoretical predictions for various colliders and c.m. energies.

- c.f. scale uncertainty at NLO $+12\% - 26\%$

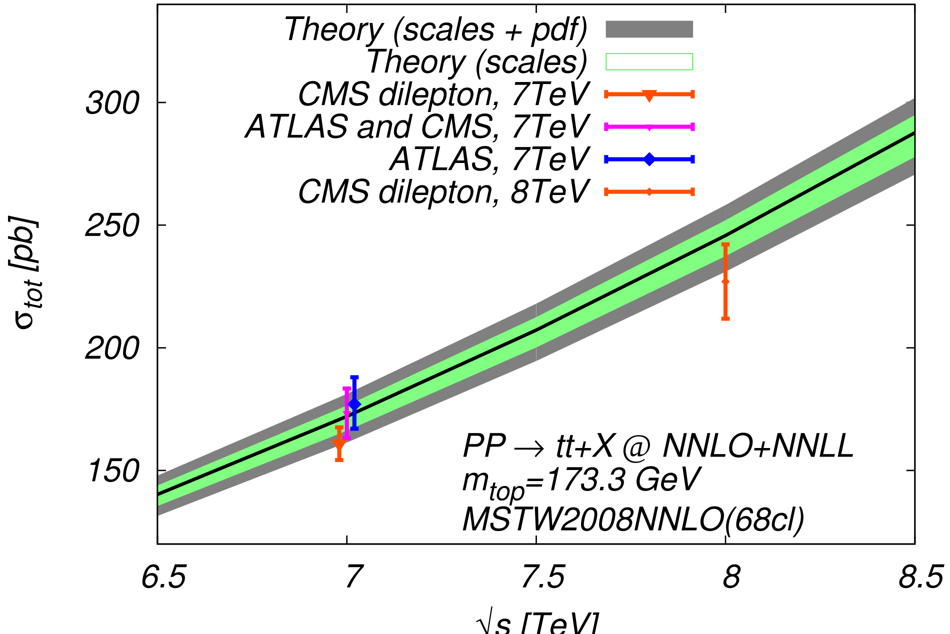

NNLO

Current status of NNLO calculations

dijets	gluon-gluon	PDFs,strong couplings,BSM	1407.5558
H+0jet	fully inclusive N3LO	Higgs couplings	1503.06056
H+1jet	fully exclusive	Higgs couplings,probing GGH vertex	1408.5325,1504.07922,1505.03893
tt pair	fully exclusive, stable tops	mass,pt, FB asymmetry,PDFs BSM	1601.05375
single top	fully exclusive, stable tops, t-channel	V_{tb},width, PDFs	1404.7116
WBF	exclusive VBF cuts	Higgs couplings	1506.02660
$W+j$	fully exclusive, decays	PDFs	1504.02131
$Z+j$	decay, off-shell effects	PDFs	1601.04569,1507.20850,1507.02850
ZH	decays to bb at NLO	Higgs couplings	1407.4747,1601.00658
WH	fully exclusive	Higgs couplings	1312.1669, 1601.00658
ZZ	fully exclusive, off-shell	trilinear gauge couplings,BSM	1405.2219, 1507.06257
WW	fully inclusive	trilinear gauge couplings,BSM	1408.5243
$W\gamma, Z\gamma$	fully exclusive	trilinear gauge couplings,BSM	1601.06751
$\gamma\gamma$	fully differential	Background studies	1110.2375,1603.02663
top decay	exclusive	Top couplings	1301.7133
$H - bb$	exclusive, massless	Higgs couplings boosted	1110.2368

NNLO top

to undertake a number of high-calibre phenomenological LHC analyses. Some examples are:

- validation of different implementations of higher-order effects in MC event generators,
- extraction of NNLO PDFs from LHC data, (especially the gluon distribution).
- improved determination of the top-quark mass
- direct measurement of the running of α_S at high scales.
- better control over background for BSM searches

Recap

- Jets are visible to the naked eye, but to use them we need a jet definition.
- Two classes of jet algorithms
- Top cross section is big; it is important to understand both as a background and as a signal
- NNLO corrections to a few processes (including top production) are becoming known.

Bibliography

- R. K. Ellis, W.J. Stirling and B.R. Webber, *QCD and Collider Physics* (Cambridge Monographs on Particle Physics, Nuclear Physics and Cosmology)
- J. Shelton, “Jet Substructure,” doi:10.1142/9789814525220_0007 arXiv:1302.0260 [hep-ph].
- G. P. Salam, “Towards Jetography,” Eur. Phys. J. C **67**, 637 (2010) doi:10.1140/epjc/s10052-010-1314-6 [arXiv:0906.1833 [hep-ph]].
- M. Cacciari, G. P. Salam and G. Soyez, “The Anti-k(t) jet clustering algorithm,” JHEP **0804**, 063 (2008) doi:10.1088/1126-6708/2008/04/063 [arXiv:0802.1189 [hep-ph]].
- J. M. Butterworth, A. R. Davison, M. Rubin and G. P. Salam, “Jet substructure as a new Higgs search channel at the LHC,” Phys. Rev. Lett. **100**, 242001 (2008) doi:10.1103/PhysRevLett.100.242001 [arXiv:0802.2470 [hep-ph]].
- P. Nason, S. Dawson and R. K. Ellis, “The Total Cross-Section for the Production of Heavy Quarks in Hadronic Collisions,” Nucl. Phys. B **303**, 607 (1988). doi:10.1016/0550-3213(88)90422-1
- M. Czakon, P. Fiedler and A. Mitov, “Total Top-Quark Pair-Production Cross Section at Hadron Colliders Through $O(\alpha_S^4)$,” Phys. Rev. Lett. **110**, 252004 (2013) doi:10.1103/PhysRevLett.110.252004 [arXiv:1303.6254 [hep-ph]].